Blockade of the BLT1-LTB4 axis does not affect mast cell migration towards advanced atherosclerotic lesions in LDLr-/- mice

Depuydt, M.A.C.; Vlaswinkel, F.D.; Hemme, E.; Delfos, L.; Bernabe Kleijn, M.N.A.; Santbrink, P.J. van; ... ; Bot, I.

scientific reports

Check for updates

OPEN

Blockade of the BLT1-LTB_4 axis does not affect mast cell migration towards advanced atherosclerotic lesions in $LDLr^{-/-}$ mice

Marie A. C. Depuydt, Femke D. Vlaswinkel, Esmeralda Hemme, Lucie Delfos, Mireia N. A. Bernabé Kleijn, Peter J. van Santbrink, Amanda C. Foks, Bram Slütter, Johan Kuiper & Ilze Bot✉

Mast cells have been associated with the progression and destabilization of advanced atherosclerotic plaques. Reducing intraplaque mast cell accumulation upon atherosclerosis progression could be a potent therapeutic strategy to limit plaque destabilization. Leukotriene B_4 (LTB_4) has been reported to induce mast cell chemotaxis in vitro. Here, we examined whether antagonism of the LTB_4-receptor BLT1 could inhibit mast cell accumulation in advanced atherosclerosis. Expression of genes involved in LTB_4 biosynthesis was determined by single-cell RNA sequencing of human atherosclerotic plaques. Subsequently, Western-type diet fed $LDLr^{-/-}$ mice with pre-existing atherosclerosis were treated with the BLT1-antagonist CP105,696 or vehicle control three times per week by oral gavage. In the spleen, a significant reduction in $CD11b^+$ myeloid cells was observed, including $Ly6C^{lo}$ and $Ly6C^{hi}$ monocytes as well as dendritic cells. However, atherosclerotic plaque size, collagen and macrophage content in the aortic root remained unaltered upon treatment. Finally, BLT1 antagonism did not affect mast cell numbers in the aortic root. Here, we show that human intraplaque leukocytes may be a source of locally produced LTB_4. However, BLT1-antagonism during atherosclerosis progression does not affect either local mast cell accumulation or plaque size, suggesting that other mechanisms participate in mast cell accumulation during atherosclerosis progression.

The mast cell, a cell type of our innate immune system that acts in the first line of defence against pathogens, has been shown to promote the development and progression of atherosclerosis. Upon activation, mast cells secrete the proteases chymase and tryptase and pro-inflammatory cytokines such as IFN-γ, which have been shown to promote atherogenesis and to lead to destabilization of the plaque[1,2]. Systemic activation of mast cells in dinitrophenyl hapten (DNP)-challenged apolipoprotein E $(apoE)^{-/-}$ mice for example resulted in an increased plaque size and incidence of intraplaque haemorrhage[1], whereas mast cell deficiency was shown to reduce atherosclerotic plaque development[2,3]. In humans, mast cells have been shown to accumulate in advanced and ruptured coronary plaques[4]. More recently, the association of mast cells with disease progression in cardiovascular disease patients was established, as significantly increased serum tryptase levels were observed in patients with acute coronary syndromes[5] and intraplaque mast cell numbers were seen to increase upon atherosclerotic plaque destabilization[6]. In addition, in that study an independent association of intraplaque mast cell numbers in carotid plaques with the incidence of clinical cardiovascular events was revealed[6]. In patients with systemic mastocytosis, a disease characterized by the accumulation of mast cells in different organs, the prevalence of cardiovascular events was increased, despite a reduction in circulating low density lipoprotein levels[7]. Together, the contribution of mast cells and their activation to atherosclerosis has been well established as has also been reviewed[8,9], however it remains elusive what factors contribute to mast cell migration towards these plaques.

Apart from various chemokines and cytokines that have been implicated in mast cell migration, lipid mediators have been described to provoke a chemotactic response in mast cells[10,11]. Leukotriene B_4 (LTB_4) is a pro-inflammatory lipid mediator well known for its chemotactic effect on myeloid and lymphoid cells[12]. Intracellular biosynthesis of LTB_4 occurs in a two-step enzymatic reaction in which arachidonic acid is metabolized by 5-lipoxygenase (5-LOX), 5-lipoxygenase activating protein (FLAP) and LTA_4 hydrolase (LTA_4H)[13]. Monocytes,

Division of BioTherapeutics, Leiden Academic Centre for Drug Research, Leiden University, Leiden, The Netherlands. ✉email: i.bot@lacdr.leidenuniv.nl

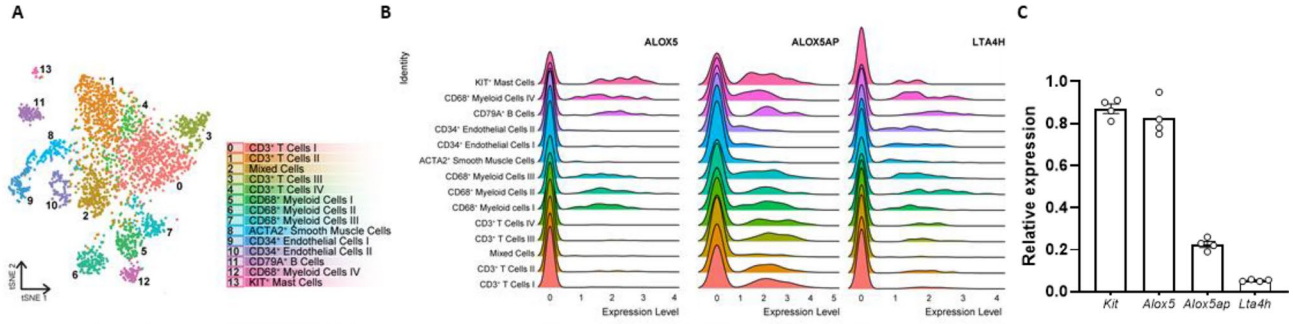

Figure 1. Expression of *ALOX5*, *ALOX5AP* and *LTA4H* in both human atherosclerotic plaque cells and murine bone-marrow derived mast cells. (**A**) Single-cell RNA sequencing of human atherosclerotic plaque cells revealed 14 distinct cell clusters, including one mast cell cluster (cluster 13)[28]. In these clusters, we measured the expression of (**B**) *ALOX5, ALOX5AP* and *LTA4H*. (**C**) Expression of *Kit*, *Alox5*, *Alox5ap* and *Lta4h* in murine bone-marrow derived mast cells. Human data n = 18; murine data: n = 4. Data represent mean ± SEM.

macrophages and mast cells are able to release LTB_4 in response to stimulation with factors such as Complement component 5a (C5a), Interleukin-1 (IL-1), Leukemia Inhibitory Factor (LIF) and Tumor Necrosis Factor α (TNFα)[14]. Synthesis and subsequent release of LTB_4 by these leukocytes will elicit a directed migration of vascular smooth muscle cells, neutrophils, eosinophils, basophils, monocytes, macrophages, dendritic cells and T cells but also of mast cell progenitors through binding with its receptor BLT1[14–20]. Previous in vitro studies showed an autocrine manner of mast cell migration towards LTB_4, which mainly recruits mast cell progenitors from the bone marrow as BLT1 expression is significantly reduced upon mast cell maturation[19].

LTB_4 and its associated mediators have been suggested to participate in atherogenesis. Heterozygous deficiency of 5-LOX for example resulted in a 95%-decrease in lesion size in Low Density Lipoprotein receptor $(LDLr)^{-/-}$ mice[21]. Moreover, BLT1 deficiency in $apoE^{-/-}$ mice resulted in decreased plaque development[15,22]. Aiello et al. showed that antagonism of BLT1 through CP105,696 caused a decrease in the infiltration of monocytes into the lesions as well as reduced monocyte activation[23]. In these studies however, the authors primarily assessed initial lesion development and the number of mast cells in these lesions was not assessed.

As mast cell numbers particularly accumulate in advanced atheromatous human plaques, it may be of therapeutic interest to identify whether the LTB_4-BLT1 axis is involved in mast cell recruitment to advanced atherosclerosis. In our study, we thus first aimed to determine whether cells in the advanced plaque are able to produce LTB_4 and next investigated whether LTB_4 participates in the chemotaxis of mast cells towards pre-established atherosclerotic plaques and would thereby contribute to further progression of the disease. Here, we administered the BLT1-antagonist CP105,696 to $LDLr^{-/-}$ mice with pre-existing atherosclerosis and analysed its effect on plaque progression. In this study, treatment with CP105,696 resulted in reduced splenic myeloid cell content, but did not affect plaque morphology and mast cell accumulation in advanced atherosclerosis.

Results

Single cell RNA sequencing reveals expression of ALOX5 on human plaque mast cells. Blockade of mast cell recruitment to atherosclerotic lesions may be a promising intervention target to reduce plaque destabilization. Mast cells have previously been described to be involved in their own recruitment[11,24], in which LTB_4 can act as an autocrine chemoattractant in multiple diseases[19,20,25,26]. Moreover, transcriptome analysis of ex vivo skin mast cells using deep-CAGE sequencing revealed expression of *ALOX5* (5-LOX), *ALOX5AP* (FLAP) and *LTA4H* (LTA_4H), the rate-limiting enzymes needed for biosynthesis of LTB_4[27]. Yet, it remains unknown whether plaque cells, among which mast cells, can produce LTB_4 in atherosclerotic lesions. In a previous study, we performed single-cell RNA sequencing on human atherosclerotic plaques obtained from carotid endarterectomy surgery from 18 patients[28]. Fourteen different cell clusters were found, of which one distinctly represented mast cells (cluster 13, Fig. 1A). Within this data set, we analysed the expression of the aforementioned genes involved in LTB_4 biosynthesis. Indeed, we observed expression of *ALOX5*, *ALOX5AP* and *LTA4H* in several myeloid cell populations, including mast cells, from human atherosclerotic plaques. Whereas *ALOX5AP* and *LTA4H* was ubiquitously expressed by all leukocytes, mast cells showed the highest expression of *ALOX5* (Fig. 1B). To assess whether these genes are also expressed in murine atherosclerotic plaques, we examined a publicly available murine single-cell RNA sequencing data set by Cochain et al.[29]. In this study, single-cell RNA sequencing was performed on $CD45^+$ cells isolated from aortas from $LDLr^{-/-}$ mice fed a chow diet, 11 weeks high fat diet and 20 weeks high fat diet, representing respectively the healthy aorta, early atherosclerotic and advanced atherosclerotic aortas. Integrating data from all three mouse models revealed 17 different clusters (Figure S1A–B). *Alox5*, *Alox5ap* and *Lta4h* were mainly found in the $Cd14^+$ $Cd68^+$ $Itgam^+$ myeloid cell clusters (Figure S1C). Therefore, we isolated all myeloid cells (clusters 0, 2, 3, 4, 6, 8, 13, 15 and 16) and examined whether expression of these three genes differed per plaque stage. *Alox5* was mainly expressed in myeloid cells of healthy aorta's compared to atherosclerotic aorta's (Figure S1D). Expression of *Alox5ap* and *Lta4h* showed no differences between plaque stages. Finally, we confirmed the expression of *Alox5*, *Alox5ap* and *Lta4h* in murine bone-marrow derived mast cells (BMMCs) (Fig. 1C). Together, these data imply that LTB_4 can be produced locally in the plaque and that

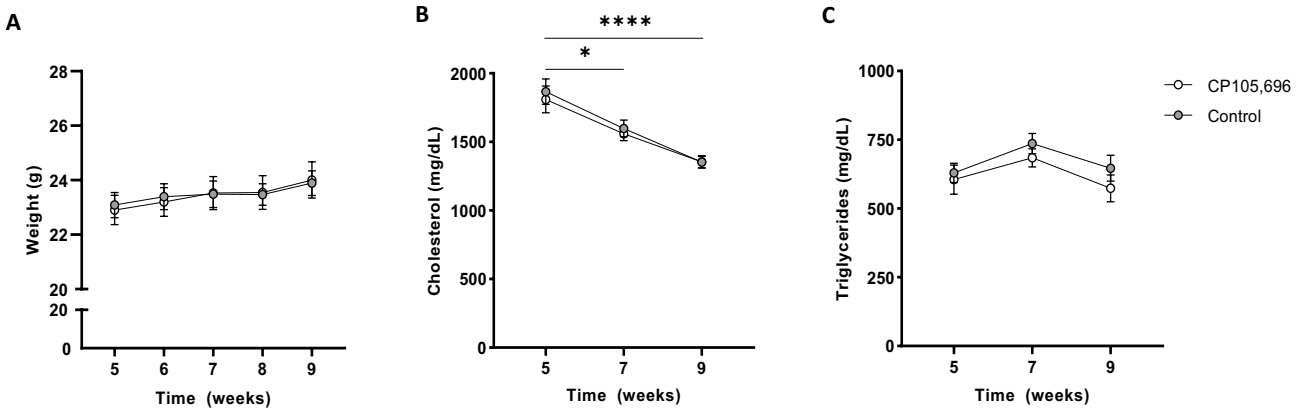

Figure 2. Body weight and plasma lipid levels upon CP105,696 treatment in LDLr$^{-/-}$ mice. (**A**) Body weight of mice was measured weekly during treatment and was not affected by CP105,696 treatment. (**B**) Plasma cholesterol and (**C**) triglyceride concentrations were obtained at t = 5, t = 7 and t = 9. $n = 15$ per group. Data represent mean ± SEM. *$p < 0.05$; ****$p < 0.0001$.

intraplaque mast cells may be its main source in the human plaque. We next aimed to determine whether blockade of the LTB_4 receptor affects mast cell migration towards the advanced atherosclerotic lesion.

CP105,696 treatment significantly lowers percentage of myeloid cells in the spleen. Next, we studied the effects of BLT1-antagonist CP105,696 treatment in our LDLr$^{-/-}$ mouse model with pre-existing atherosclerosis (Fig. S2). CP105,696 treatment did not affect total body weight throughout the experiment (t = 9 weeks, Control: 24.0 ± 0.7 g vs. CP105,696: 23.9 ± 0.5 g; Fig. 2A). Serum total cholesterol levels were decreased in both groups during treatment (w5 vs. w9, Control: 1809.7 ± 98.6 mg/dL vs. 1354.8 ± 44.1 mg/dL, $p = 0.0002$ and CP105,696: 1866.2 ± 92.2 mg/dL vs. 1351.9 ± 42.7 mg/dL, $p = 0.00002$), but no differences were found between control and CP105,696 (Fig. 2B). The decline in cholesterol level can be ascribed to the Tween 80 in the solvent as polysorbates were previously reported to induce cholesterol lowering[30]. No differences in serum triglyceride levels were detected (Fig. 2C).

The BLT1-LTB_4 axis has previously been described to affect migration of multiple myeloid cells, including monocytes and dendritic cells[31]. To confirm that CP105,696 inhibited the BLT1 receptor in vivo, we used flow cytometry to measure myeloid subsets in blood and spleen. In the circulation, no differences were found in the total percentage of myeloid cells (CD11b$^+$; Fig. 3A). The percentage of the different monocyte subtypes (CD11b$^+$Ly6C^{hi}, CD11b$^+$Ly6C^{mid} and CD11b$^+$Ly6C^{lo}) and of CD11b$^+$CD11c$^+$ cells, which predominantly characterize dendritic cells, also remained unaltered upon treatment (Fig. 3B–E). In the spleen we observed a clear effect of treatment with the BLT1-antagonist. The percentage of total myeloid cells was significantly reduced upon treatment with CP105,696 (Control: 11.3 ± 0.48% vs CP105,696: 9.4 ± 0.56%; $p = 0.016$; Fig. 3F). Both the percentage of inflammatory monocytes (Ly6C^{hi}; Control: 0.96 ± 0.067% vs. CP105,696: 0.69 ± 0.069%; $p = 0.011$; Fig. 3G,K) and that of the patrolling monocytes (Ly6C^{lo}; Control: 0.80 ± 0.032 vs. CP105,696: 0.71 ± 0.36; $p = 0.07$; Fig. 3I,K) showed respectively a significant decrease and a trend towards a decrease after BLT1 inhibition, whereas Ly6C^{int} monocyte levels did not differ between groups (Fig. 3H,K). Furthermore, we observed a reduced accumulation of CD11b$^+$CD11c$^+$ dendritic cells in the spleen of treated mice (Control: 4.8 ± 0.16 vs. CP105,696: 4.2 ± 0.17; $p = 0.016$; Fig. 3J).

Treatment with CP105,696 did not affect plaque progression in advanced atherosclerosis. Next, we assessed whether BLT1-antagonism affected the size and morphology of advanced lesions. CP105,696 treatment did not affect aortic root plaque area (Control: 3.7 ± 0.3*10^5 µm^2 vs. CP105,696: 3.9 ± 0.2*10^5 µm^2; $p = 0.60$) and the percentage of Oil Red O staining in the plaque (Control: 34.5 ± 3.3% vs. CP105,696: 32.3 ± 5.1%; $p = 0.18$; Fig. 4A). The degree of stenosis (Control: 36 ± 2% vs. CP105,696: 39 ± 1%; $p = 0.233$) as well as the total lesion area and plaque volume (Control: 1212 ± 86*10^5 µm^3 vs. CP105,696: 1264 ± 64*10^5 µm^3; $p = 0.633$) were unaltered by BLT1 antagonism (Figure S3A–C). We also examined collagen content and necrotic core size by Sirius Red staining. Both parameters did not change upon treatment with CP105,696 (Fig. 4B). Furthermore, no differences in macrophage content were observed between the groups (Fig. 4C). In addition, flow cytometry analysis of the atherosclerotic aortic arch did not reveal any differences in the percentage of live CD45$^+$ leukocytes of the single cell population and the percentage of total lymphocytes in the CD45$^+$ cell population (data not shown) between the groups. Also, the percentage of CD11b$^+$ myeloid cells and that of CD11b$^+$CD11c$^+$ dendritic cells in the CD45$^+$ cell population (Figure S4A–C) were not affected by CP105,696 treatment. Thus, BLT1-antagonism did not affect plaque morphology or myeloid cell content in a model of pre-existing atherosclerosis.

No difference in mast cell accumulation in the aortic root upon BLT1-antagonism. Subsequently, we aimed to investigate whether LTB_4 is a chemoattractant for the recruitment of mast cells towards

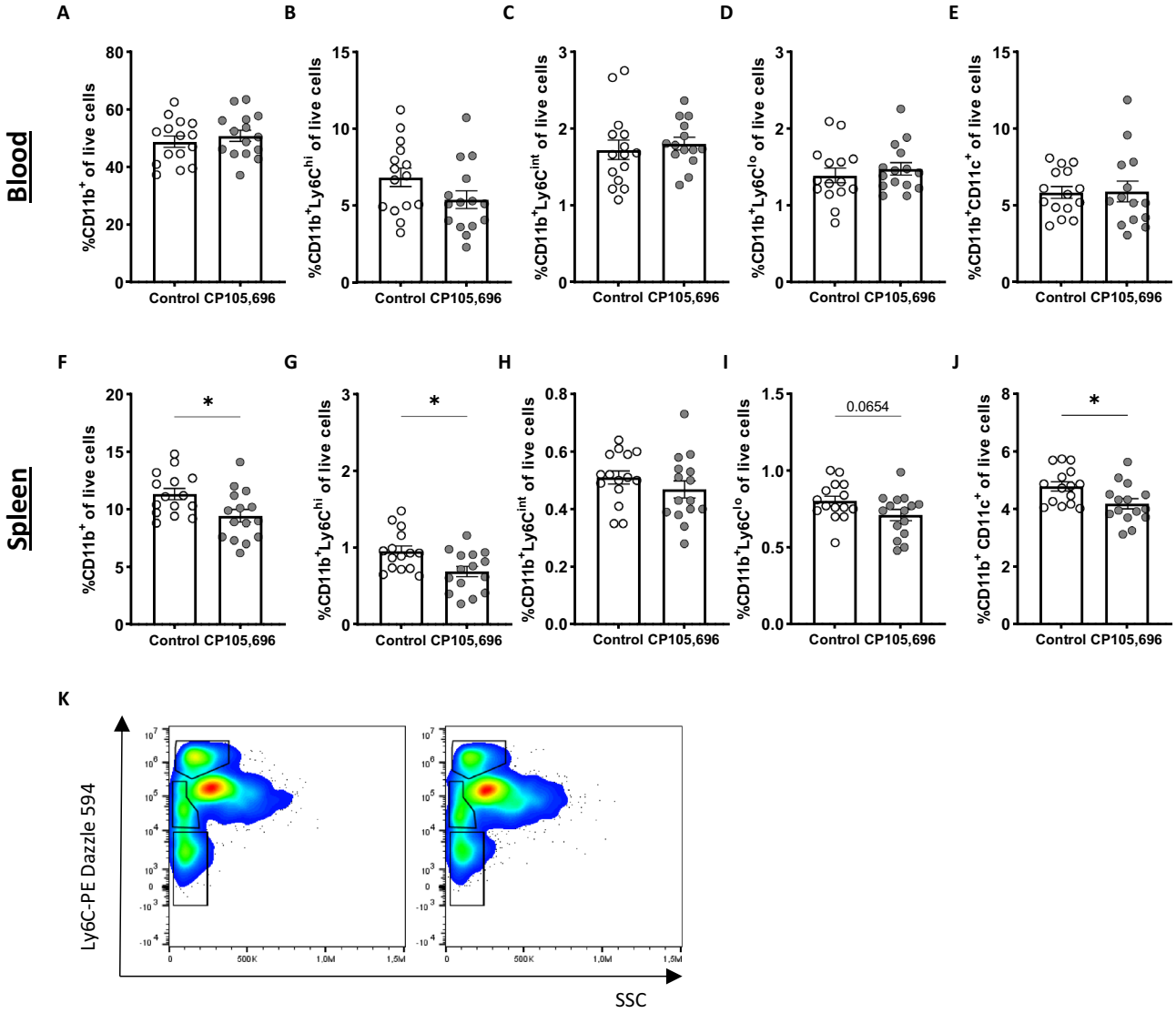

Figure 3. Myeloid cells significantly decreased with BLT1-antagonism in the spleen. Upon sacrifice, blood and spleen were collected and processed to obtain a single cell suspension for flow cytometry analysis. In the blood, the percentage of (**A**) $CD11b^+$ myeloid cells, (**B**) $Ly6C^{hi}$ monocytes, (**C**) $Ly6C^{int}$ monocytes, (**D**) $Ly6C^{lo}$ monocytes and (**E**) $CD11b^+CD11c^+$ dendritic cells was not different between the CP105,696 treated and the control group. In the spleen, a significant reduction in the percentage of (**F**) $CD11b^+$ myeloid cell content was found with CP105,696 treatment. Specifically, BLT1-antagonism resulted in a decrease in (**G**) the percentage of $CD11b^+Ly6C^{hi}$ monocytes, no difference in (**H**) the percentage of $CD11b^+Ly6C^{int}$ monocytes and (**I**) a trend towards a decrease in the percentage of $CD11b^+Ly6C^{lo}$ monocytes. (**J**) Furthermore, we observed a significant decrease in the percentage of $CD11b^+$ $CD11c^+$ dendritic cells. (**K**) Representative Flow Cytometry plot of monocytes in the spleen, left: control, right: CP105,696. $n = 14–15$ per group. Data represent mean ± SEM. $^*p < 0.05$.

the atherosclerotic plaque. We first assessed the percentage of mast cell progenitors (MCps) in blood and thereby examined whether BLT1-antagonism affected their migration. No differences were observed in $CD34^+Lin^-CD127^-CD16/32^+CD117^+FC\varepsilon RI^+$ MCps in blood between groups (Control: 0.010 ± 0.002% vs. CP105,696: 0.012 ± 0.002%; $p = 0.34$; Fig. 5A). We also determined mast cell numbers in the aortic root of treated and non-treated mice. In line with the data on mast cell progenitors, no differences were found in total mast cell numbers (Control: 16.0 ± 1.5 mast cells/mm^2 vs. CP105,696: 16.5 ± 1.3 mast cells/mm^2; $p = 0.80$; Fig. 5B,D) and in the percentage of activated mast cells (Control: 46 ± 2% vs. CP105,696: 51 ± 2%; $p = 0.12$; Fig. 5C) in the aortic root.

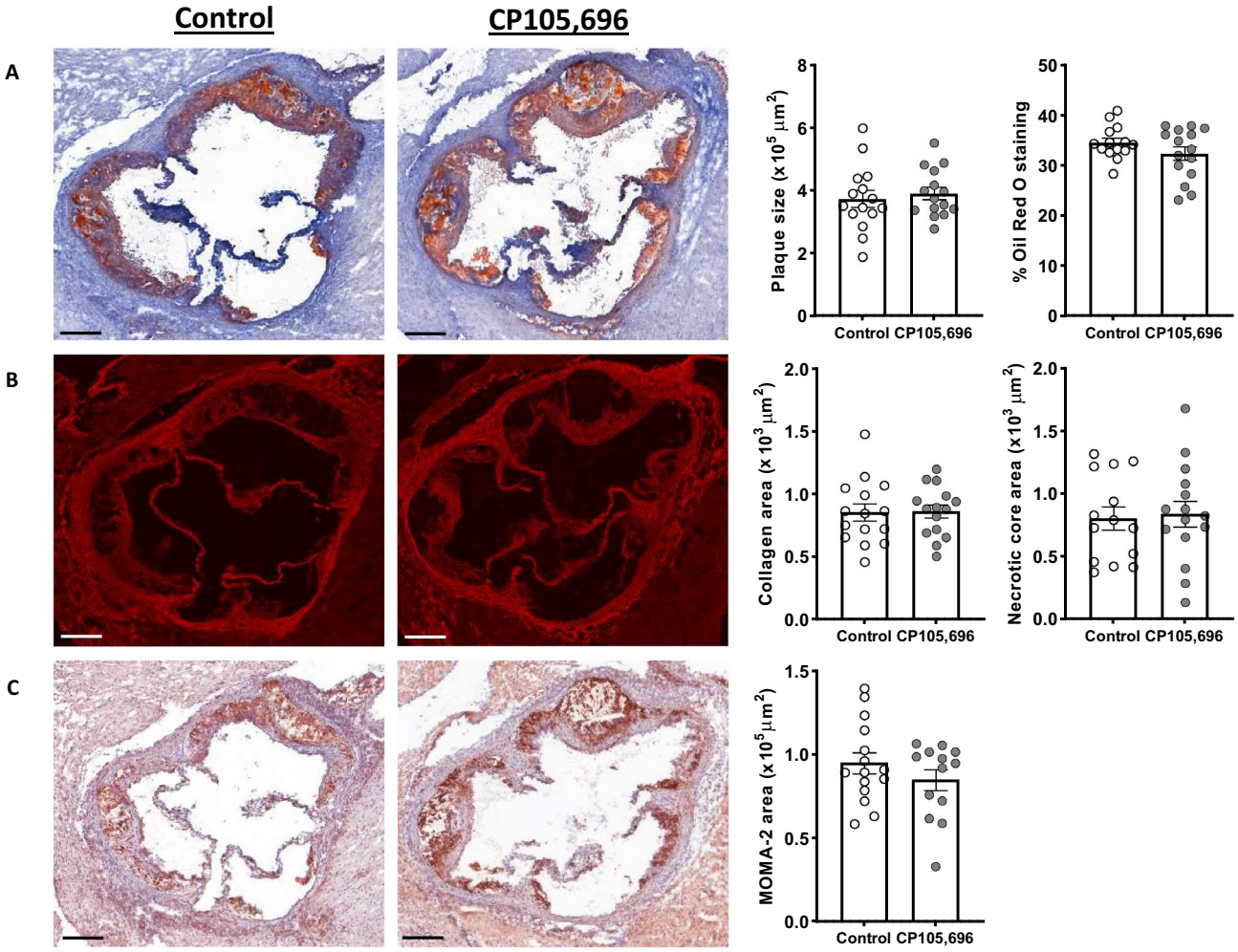

Figure 4. Inhibition of the BLT1-LTB$_4$ axis did not alter plaque morphology in advanced atherosclerosis. (**A**) Atherosclerotic plaque size and percentage Oil Red O staining in the plaque did not differ upon treatment with CP105,696 as assessed by Oil-Red O staining of the aortic root. (**B**) Sirius red staining of the aortic root did not reveal differences in plaque collagen and necrotic core area in CP105,696 treated mice versus controls. (**C**) BLT1-antagonism did not affect the MOMA-2 macrophage area in the aortic root. All representative pictures are taken at optical magnification 5x; the bar indicates 200 µm. n = 13–15 per group. Data represent mean ± SEM.

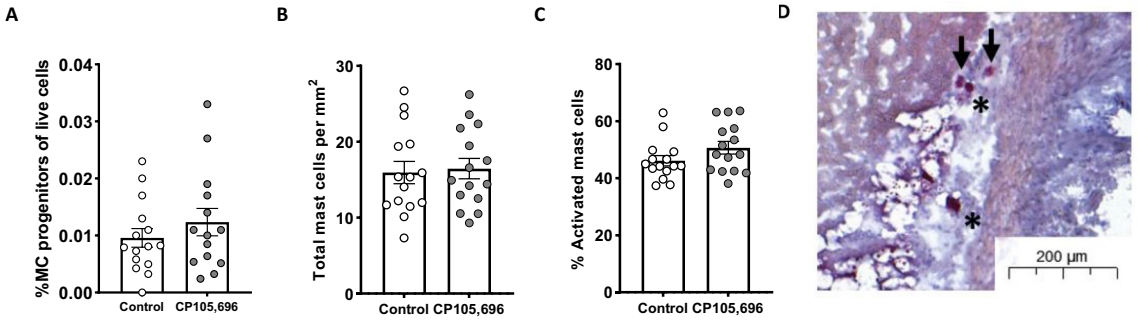

Figure 5. Mast cell accumulation in advanced atherosclerotic plaques (**A**) BLT1-antagonism did not affect the percentage of CD34$^+$Lin$^-$CD127$^-$CD16/32$^+$CD117$^+$FCεRI$^+$ mast cell progenitors in blood. (**B**) The total number of mast cells per mm^2 perivascular tissue of the aortic root tissue and (**C**) the percentage of activated mast cells did not differ between the CP105,696 treated and control group. (**D**) Representative image of mast cell staining in the aortic root section. Asterix indicates resting mast cells, arrows indicate activated mast cells. n = 14–15 per group. Data represent mean ± SEM.

Discussion

Mast cells actively contribute to progression and destabilization of advanced atherosclerotic lesions. Prevention of mast cell recruitment to the atherosclerotic lesion could thus be a promising therapeutic strategy to limit plaque destabilization. In this study, we aimed to investigate whether inhibition of the BLT1-LTB_4 axis via BLT1-antagonism limits mast cell accumulation in advanced atherosclerosis and via this way prevent plaque instability. Although we observed expression of genes involved in LTB_4 biosynthesis in the human atherosclerotic plaque, including prominent expression in mast cells, inhibition of BLT1 in vivo did not affect plaque morphology and the number of mast cells in the advanced atherosclerotic plaque.

The LTB_4 biosynthesis pathway has previously been examined in atherosclerosis. ALOX5 (5-LOX), ALOX5AP (FLAP) and LTA_4H have been found to be expressed in human atherosclerotic plaques, and were generally seen to colocalize with macrophages[32–34]. As we show here, these genes are also detected in the murine single-cell RNA sequencing data[29], while protein expression of ALOX5 and LTA_4H has been established in murine plaques and adventitial macrophages as well[34]. These proteins have also been targeted in experimental atherosclerosis studies. Similar to CP105,696, promising effects on atherosclerosis development have been shown with FLAP inhibitors like MK-886 and BAYx1005[35,36] Studies examining 5-LOX in atherosclerosis have been less evident. 5-LOX deficiency alone was not sufficient to limit atherosclerosis development, only in combination with 12–15-LO deficiency an effect was observed[37]. Furthermore, in humans, 5-LOX inhibition using VIA-2291 gave rather conflicting results. Gaztanaga et al. reported that treatment with VIA-2291 was not associated with significant reductions in vascular inflammation in patients after an acute coronary syndrome, while Matsumoto et al. showed that VIA-2291 resulted in slower plaque progression as measured by CT-angiography[38,39]. It must be noted that all experimental studies in mice focussed on the effects of treatment during lesion initiation. As our single-cell RNA sequencing data of advanced human plaques revealed that mast cells have high expression of the LTB_4 biosynthesis-related genes, we aimed to examine the effect of LTB_4 inhibition in advanced atherosclerosis.

In our study, we observed a significant reduction in splenic myeloid cells, of which the most pronounced effects were found on both the inflammatory and patrolling monocyte subsets as well as on dendritic cells. This may be a result of direct inhibition of BLT1 on these cell subsets, but may also be indirectly related as LTB_4 has previously been shown to upregulate Monocyte Chemoattractant Protein (MCP-) 1[40]. Huang et al. showed that in human monocytes, LTB_4 interacts with BLT1 to upregulate mRNA expression and active synthesis of MCP-1 by monocytes to induce a feed-forward amplification loop for their chemotaxis[41]. Furthermore, it was shown that LTB_4 induced increased avidity and/or affinity of β1-integrin and β2-integrin to their endothelial ligands, further stimulating firm arrest of monocytes under physiologic flow[42]. Moreover, in both studies pharmacological inhibition of the LTB_4-BLT1 axis abrogated these effects. In line with these reported findings, CP105,696 reduced splenic myeloid cell and dendritic cell levels, of which the most pronounced effects were found on inflammatory and patrolling monocytes, which both have been found to migrate towards MCP-1[43,44].

In atherosclerosis, BLT1 has already been a target in multiple studies. In line with the chemotactic effects on monocytes, Heller et al. showed that BLT1 deficiency resulted in a significant reduction in lesion size as well as macrophage content in apoE deficient mice[15]. Furthermore, in both apoE and LDLr deficient mice, a 35-day treatment with BLT1-antagonist CP105,696 led to a significant reduction in plaque size and $CD11b^+$ cells in the circulation[23]. In these studies however, intervention in the LTB1-BLT_4 axis occurred immediately upon lesion initiation. As mast cells are known to accumulate in later stages of disease[6,9], we aimed to assess the effect of BLT1 blockade on pre-existing plaques. However, we did not observe any differences in plaque morphology as neither plaque and necrotic core size, nor plaque collagen and macrophage content were affected by BLT1 antagonism. Furthermore, flow cytometry analysis of the atherosclerotic aortic arch did not reveal any effects on total leukocyte and myeloid cell content upon CP105,696 treatment. Apparently, blockade of BLT1 is not sufficient to affect plaque size and composition at this stage of the disease. Indeed, Aiello et al. described that more distinct effects of CP105,696 were observed in $apoE^{-/-}$ mice of 15 weeks old, with smaller and thus less complex lesions as compared to 24 weeks old mice with more advanced atherosclerosis[23]. In addition, in a $BLT1^{-/-}apoE^{-/-}$ mouse model on a western type diet, differences in lesion size were only detected after 4 weeks of diet, whereas after 8 weeks and 19 weeks of diet, lesion size was similar in both $BLT1^{-/-}apoE^{-/-}$ and $apoE^{-/-}$ mice[22]. This may be explained by the fact that monocyte influx into the plaque is a less dominant mechanism in advanced atherosclerosis as compared to early atherogenesis. In addition, macrophage egress has been shown to decrease with atherosclerosis progression[45,46]. Combined, this results in differences in myeloid cell dynamics between early and advanced atherosclerosis and effects observed upon BLT1-antagonism may thus be disease stage specific. Alternatively, in later stages of disease, other factors in the plaque microenvironment may contribute to the recruitment of different cell types to the plaque, which means that the decrease in myeloid content in the spleen due to BLT1-antagonism may not directly translate into effects in the plaque.

LTB_4 has previously been described to induce directed migration of mast cells and their progenitors[20]. In vitro, LTB_4 eluted from the supernatant of activated BMMCs elicited chemotaxis of immature mast cells. In mice, increased recruitment of CMFDA-labelled mast cell progenitors was detected upon injection of LTB_4 into the dorsal skin. LTB_4 was shown to be a potent chemoattractant for immature $c\text{-}kit^+$ human umbilical cord blood-derived mast cells (CBMCs), whereas mature $c\text{-}kit^+$ mast cells remained unresponsive[19]. Nevertheless, in our study we did not observe any differences in the percentage of circulating mast cell progenitors after 4 weeks of treatment with CP105,696. Moreover, the total number of mast cells and the percentage of activated mast cells in the aortic root also remained unaffected, suggesting that LTB_4 does not act as a chemoattractant for mast cells in advanced atherosclerosis via the LTB_4 receptor BLT1. Assessment of mast cell accumulation in other sites of advanced atherosclerosis may be warranted to confirm our findings. In vitro cultured murine and human mast cells have however also shown expression of the LTB_4 low affinity receptor BLT2. Lundeen et al. showed that inhibition with a selective BLT2 antagonist dose-dependently reduced migration of mast cells towards LTB_4 in vitro,

suggesting that this interaction of BLT2 and LTB_4 could be involved in mast cell chemotaxis[20]. As CP105,696 is a selective BLT1-antagonist, we cannot exclude BLT2-induced mast cell recruitment towards the plaque in our experiment. Future studies may aim to investigate whether BLT2 is involved in mast cell chemotaxis to the advanced plaque independent of BLT1.

Although we did not see any differences in mast cell recruitment towards the atherosclerotic plaque in CP105,696 treated mice compared to our controls, single-cell RNA sequencing of human carotid atherosclerotic lesions suggests that mast cells may contribute to the local LTB_4 concentrations in the plaque as intraplaque mast cells highly expressed genes involved in LTB_4 biosynthesis. Interestingly, *ALOX5*, encoding for 5-LOX, was most prominently expressed in intraplaque mast cells as compared to other plaque cell types. In line, Spanbroek et al. showed that 5-LOX colocalized with tryptase$^+$ mast cells in carotid arteries and that the number of 5-LOX expressing cells increased in later stages of disease[47]. Furthermore, 5-LOX expression was mainly found in the shoulder regions of atherosclerotic lesions[48], where mast cells have also been shown to reside and accumulate[49]. Together, this suggest that although mast cells may not induce an autocrine loop for their recruitment towards murine atherosclerotic lesions, that they may induce migration of other leukocytes towards the lesion via LTB_4. We cannot exclude species-induced differences here, however based on current literature, we do not expect any differences as both mouse and human mast cells in culture were seen to migrate towards LTB_4[19,20].

To conclude, here we show that BLT1-antagonism does not affect plaque size and morphology during advanced stages of atherosclerosis, which suggests that LTB_4 is not involved in the progression of advanced atherosclerotic lesions. Moreover, we show that LTB_4 does not seem to be involved in mast cell migration towards atherosclerotic plaques, but that mast cells are able contribute to local LTB_4 production in the lesion. To identify novel therapeutic intervention strategies, further research should be aimed at the elucidation of mechanisms that induce directed migration of mast cells towards the advanced atherosclerotic plaque.

Methods

Single-cell RNA sequencing. Human carotid artery plaques were collected from 18 patients (14 male, 4 female) that underwent carotid endarterectomy surgery as part of AtheroExpress, an ongoing biobank study at the University Medical Centre Utrecht (Study approval number TME/C-01.18, protocol number 03/114)[50]. Single cells were obtained and processed for single-cell RNA sequencing as previously described[28]. All studies were performed in accordance with the Declaration of Helsinki. Informed consent was obtained from all subjects involved in the study. Murine single-cell RNA sequencing data sets were obtained from Cochain et al.[29] and processed as previously described[51,52]. Briefly, data sets were processed using the SCTransform normalization method[53], integrated using rpca reduction and subsequently clustered, all according to the Seurat "scRNA-seq integration" vignette[54]. All data analyses were executed in R-4.0.2.

Animals. All animal experiments were performed in compliance with the guidelines of the Dutch government and the Directive 2010/63/EU of the European Parliament. The experiment was approved by the Ethics Committee for Animal Experiments and the Animal Welfare Body of Leiden University (Project 106002017887, Study number 887, 1–103).

Female 7–10 week old $LDLr^{-/-}$ mice (C57BL/6 background) (n = 15/group) that were bred in-house were provided with food and water ad libitum. From the start of the experiment, the mice were fed a cholesterol-rich western-type diet (0.25% cholesterol, 15% cocoa butter, Special Diet Services, Essex, UK), which continued for 9 weeks in total. At week 5, the mice were randomized in groups based on age, weight and serum cholesterol levels. Previous work from our group showed that mast cell accumulation in the aortic root starts at approximately 6 weeks after the start of western-type diet feeding[55]. Therefore, from week 5 onwards, mice received either 20 mg/kg of BLT1-antagonist CP105,696 (Sigma-Aldrich) or vehicle control (0.6% Tween 80, 0.25% methylcellulose in phosphate-buffered saline (PBS)) three times per week via oral gavage for 4 weeks (n = 15 per group). A detailed schedule of the experimental setup is provided in Figure S2. Blood was drawn by tail vein bleeding at week 5 and week 7. At week 9, the mice were sacrificed upon subcutaneous administration of anaesthetics (ketamine (40 mg/mL), atropine (0.1 mg/mL) and xylazine (8 mg/mL)). Blood was collected via orbital bleeding, after which the mice were perfused with PBS through the left cardiac ventricle. Next, organs were collected for analysis.

Cholesterol and triglyceride assay. Serum was collected through centrifugation at 8000 rpm for 10 min at 4 °C and stored at − 80 °C until further use. Total cholesterol levels were determined through an enzymatic colorimetric assay (Roche/Hitachi, Mannheim, Germany). Triglyceride levels in serum were measured by an enzymatic colorimetric assay (Roche Diagnostics). For both assays, Precipath standardized serum (Roche Diagnostics) was used as an internal standard.

Cell isolation. Blood samples were lysed with ACK lysis buffer (0.15 M NH_4Cl, 1 mM $KHCO_3$, 0.1 mM Na_2EDTA, pH 7.3) to obtain a single white blood cell suspension. Spleens were passed through a 70 µm cell strainer (Greiner, Bio-one, Kremsmunster, Austria) and splenocytes were subsequently lysed with ACK lysis buffer. Aortic arches were cut into small pieces and enzymatically digested in a digestion mix containing collagenase I (450 U/mL), collagenase XI (250 U/mL), DNAse (120 U/mL), and hyaluronidase (120 U/mL; all Sigma–Aldrich) for 30 min at 37 °C while shaking. After incubation, all samples were passed through a 70 µm cell strainer (Geiner, Bio-one, Kremsmunster, Austria). Single cell suspensions were then used for flow cytometry analysis.

Flow cytometry. Single cell suspensions from blood and spleen were extracellularly stained with a mixture of selected fluorescent labelled antibodies for 30 min at 4 °C. The antibodies used for flow cytometry are listed

in Table S1. All measurements were performed on a Cytoflex S (Beckman and Coulter, USA) and analysed with FlowJo v10.7 (Treestar, San Carlos, CA, USA).

Histology. After euthanasia, the hearts were dissected, embedded and frozen in Tissue-Tek OCT compound (Sakura). 10 µm cryosections of the aortic root were prepared for histological analysis. Mean plaque size and the percentage plaque area of total vessel area (vessel occlusion) were assessed by Oil-Red-O (ORO) staining. From the first appearance of the three aortic valves, 5 consecutive slides with 80 µm distance between the sections were analysed for total lesion size within the three valves, after which the average lesion size was calculated. Average lesion size was also calculated in relation to distance from the start of the three-valve area. Subsequently, plaque volume was calculated as area under the curve. Collagen content of the plaque was measured using a Sirius Red staining after which fluorescent staining of three section per mouse was analysed and averaged. Similarly, the average necrotic core size was measured using the Sirius Red staining by measuring the acellular debris-rich areas of the plaque of three sections per mouse. Macrophage content was determined by using MOMA-2 antibody (1:1000; rat IgG2b; Bio-Rad). Naphthol AS-D chloroacetate staining (Sigma-Aldrich) was performed to manually quantify resting and activated mast cells in the plaques. Mast cells were identified and counted in the perivascular tissue of the aortic root at the site of atherosclerosis. A mast cell was considered resting when all granula were maintained inside the cell, while mast cells were assessed as activated when granula were deposited in the tissue surrounding the mast cell. Sections were digitalised using a Panoramic 250 Flash III slide scanner (3DHISTECH, Hungary). Analysis was performed using ImageJ software.

Cell Culture. Bone marrow-derived mast cells (BMMCs) from 7 to 10 weeks $LDLr^{-/-}$ mice were cultured in RPMI 1640 containing 25 mM HEPES (Lonza) and supplemented with 10% fetal calf serum, 1% L-glutamine (Lonza), 100 U/mL mix of penicillin/streptomycin (PAA), 1% sodium pyruvate (Sigma-Aldrich), 1% non-essential amino acids (MEM NEAA; Gibco) and 5 ng/mL IL-3 (Immunotools). Cells were incubated at 37 °C and 5% CO_2 and were kept at a density of $0.25*10^6$ cells per mL by weekly subculturing. BMMCs were cultured for 4 weeks in total to obtain mature mast cells.

RNA isolation and gene expression analysis. RNA isolation from $1*10^6$ mast cells was performed using the guanine isothiocyanate method[56]. Using RevertAid M-MuLV reverse transcriptase cDNA was isolated according to the manufacturer's instructions. Quantitative gene expression analysis was performed with the SYBR Green Master Mix technology on a QuantStudio 6 Flex (Applied Biosystems by Life Technologies). A list of qPCR primers can be find in Table S2.

Statistical analysis. The data are presented as mean ± SEM and analysed in GraphPad Prism 9. Shapiro-Wilkson normality test was used to test data for normal distribution. Outliers were identified by a Grubbs' test. Data was analysed using an unpaired two-tailed Student *t*-test or Mann–Whitney test. $p < 0.05$ was considered to be significant.

Ethics declarations. All experiments have been performed in accordance with the ARRIVE guidelines.

Human samples The study was conducted according to the guidelines of the Declaration of Helsinki, and approved by the Medical Ethical Committee of the University Medical Centre Utrecht (UMCU). All samples were included in the Athero-Express Study (www.atheroexpress.nl), an ongoing biobank study at the UMCU. Informed consent was obtained from all subjects involved in the study.

Animal studies: All animal experiments were performed in compliance with the guidelines of the Dutch government and the Directive 2010/63/EU of the European Parliament. The experiment was approved by the Ethics Committee for Animal Experiments and the Animal Welfare Body of Leiden University (project 106,002,017,887, study number 887,1–103).

Data availability

The data presented in this study are available on request from the corresponding author. The human scRNAseq data presented in this study are retrieved from Depuydt et al. Circ Res. 2020[28]. R scripts are available on GitHub (https://github.com/AtheroExpress/MicroanatomyHumanPlaque_scRNAseq). Other data is available upon request from the corresponding authors of this paper.

Received: 20 June 2022; Accepted: 26 October 2022
Published online: 01 November 2022

References

1. Bot, I. *et al.* Perivascular mast cells promote atherogenesis and induce plaque destabilization in apolipoprotein E-deficient mice. *Circulation* **115**, 2516–2525 (2007).
2. Sun, J. *et al.* Mast cells promote atherosclerosis by releasing proinflammatory cytokines. *Nat. Med.* **13**, 719–724 (2007).
3. Heikkilä, H. M. *et al.* Mast cells promote atherosclerosis by inducing both an atherogenic lipid profile and vascular inflammation. *J. Cell. Biochem.* **109**, 615–623 (2010).
4. Laine, P. *et al.* Association between myocardial infarction and the mast cells in the adventitia of the infarct-related coronary artery. *Circulation* **99**, 361–369 (1999).
5. Morici, N. *et al.* Mast cells and acute coronary syndromes: relationship between serum tryptase, clinical outcome and severity of coronary artery disease. *Open Hear.* **3**, (2016).
6. Willems, S. *et al.* Mast cells in human carotid atherosclerotic plaques are associated with intraplaque microvessel density and the occurrence of future cardiovascular events. *Eur. Heart J.* **34**, 3699–3706 (2013).

7. Indhirajanti, S. *et al.* Systemic mastocytosis associates with cardiovascular events despite lower plasma lipid levels. *Atherosclerosis* **268**, 152–156 (2018).
8. Hermans, M., Van Lennep, J. R., Van Daele, P. & Bot, I. Mast Cells in Cardiovascular Disease: From Bench to Bedside. *Int. J. Mol. Sci.* **20**, 3395 (2019).
9. Kovanen, P. T. & Bot, I. Mast cells in atherosclerotic cardiovascular disease—Activators and actions. *Eur. J. Pharmacol.* **816**, 37–46 (2017).
10. Collington, S. J., Williams, T. J. & Weller, C. L. Mechanisms underlying the localisation of mast cells in tissues. *Trends Immunol.* **32**, 478–485 (2011).
11. Halova, I., Draberova, L. & Draber, P. Mast cell chemotaxis—Chemoattractants and signaling pathways. *Front. Immunol.* **3**, (2012).
12. Funk, C. D. Prostaglandins and leukotrienes: advances in eicosanoid biology. *Science* **294**, 1871–1875 (2001).
13. Wan, M., Tang, X., Stsiapanava, A. & Haeggström, J. Z. Biosynthesis of leukotriene B 4. *Semin. Immunol.* **33**, 3–15 (2017).
14. Subramanian, B. C., Majumdar, R. & Parent, C. A. The role of the LTB 4-BLT1 axis in chemotactic gradient sensing and directed leukocyte migration. *Semin. Immunol.* **33**, 16–29 (2017).
15. Heller, E. A. *et al.* Inhibition of atherogenesis in BLT1-deficient mice reveals a role for LTB4 and BLT1 in smooth muscle cell recruitment. *Circulation* **112**, 578–586 (2005).
16. Yokomizo, T. Two distinct leukotriene B4 receptors, BLT1 and BLT2. *J. Biochem.* **157**, 65–71 (2015).
17. Tager, A. M. *et al.* Leukotriene B4 receptor BLT1 mediates early effector T cell recruitment. *Nat. Immunol.* **4**, 982–990 (2003).
18. Koga, T. *et al.* Expression of leukotriene B 4 receptor 1 defines functionally distinct DCs that control allergic skin inflammation. *Cell. Mol. Immunol.* **18**, 1437–1449 (2021).
19. Weller, C. L. *et al.* Leukotriene B4, an activation product of mast cells, is a chemoattractant for their progenitors. *J. Exp. Med.* **201**, 1961–1971 (2005).
20. Lundeen, K. A., Sun, B., Karlsson, L. & Fourie, A. M. Leukotriene B4 receptors BLT1 and BLT2: expression and function in human and murine mast cells. *J. Immunol.* **177**, 3439–3447 (2006).
21. Mehrabian, M. *et al.* Identification of 5-lipoxygenase as a major gene contributing to atherosclerosis susceptibility in mice. *Circ. Res.* **91**, 120–126 (2002).
22. Subbarao, K. *et al.* Role of leukotriene B4 receptors in the development of atherosclerosis: potential mechanisms. *Arterioscler. Thromb. Vasc. Biol.* **24**, 369–375 (2004).
23. Aiello, R. J. *et al.* Leukotriene B4 receptor antagonism reduces monocytic foam cells in mice. *Arterioscler. Thromb. Vasc. Biol.* **22**, 443–449 (2002).
24. Jamur, M. C. & Oliver, C. Origin, maturation and recruitment of mast cell precursors. *Front. Biosci. (Schol. Ed).* **3**, 1390 (2011).
25. Miyahara, N. *et al.* Leukotriene B4 release from mast cells in IgE-mediated airway hyperresponsiveness and inflammation. *Am. J. Respir. Cell Mol. Biol.* **40**, 672–682 (2009).
26. Ohnishi, H., Miyahara, N. & Gelfand, E. W. The role of leukotriene B(4) in allergic diseases. *Allergol. Int.* **57**, 291–298 (2008).
27. Motakis, E. *et al.* Redefinition of the human mast cell transcriptome by deep-CAGE sequencing. *Blood* **123**, e58-67 (2014).
28. Depuydt, M. A. C. *et al.* Microanatomy of the human atherosclerotic plaque by single-cell transcriptomics. *Circ. Res.* **127**, 1437–1455 (2020).
29. Cochain, C. *et al.* Single-cell RNA-Seq reveals the transcriptional landscape and heterogeneity of aortic macrophages in murine atherosclerosis. *Circ. Res.* **122**, 1661–1674 (2018).
30. Li, X. *et al.* Polysorbates as novel lipid-modulating candidates for reducing serum total cholesterol and low-density lipoprotein levels in hyperlipidemic C57BL/6J mice and rats. *Eur. J. Pharmacol.* **660**, 468–475 (2011).
31. Shin, E. H., Lee, H. Y. & Bae, Y. S. Leukotriene B4 stimulates human monocyte-derived dendritic cell chemotaxis. *Biochem. Biophys. Res. Commun.* **348**, 606–611 (2006).
32. Cipollone, F. *et al.* Association between 5-lipoxygenase expression and plaque instability in humans. *Arterioscler. Thromb. Vasc. Biol.* **25**, 1665–1670 (2005).
33. Zhou, Y. J. *et al.* Expanding expression of the 5-lipoxygenase/leukotriene B4 pathway in atherosclerotic lesions of diabetic patients promotes plaque instability. *Biochem. Biophys. Res. Commun.* **363**, 30–36 (2007).
34. Qiu, H. *et al.* Expression of 5-lipoxygenase and leukotriene A4 hydrolase in human atherosclerotic lesions correlates with symptoms of plaque instability. *Proc. Natl. Acad. Sci. USA* **103**, 8161–8166 (2006).
35. Jawien, J. *et al.* Inhibition of five lipoxygenase activating protein (FLAP) by MK-886 decreases atherosclerosis in apoE/LDLR-double knockout mice. *Eur. J. Clin. Invest.* **36**, 141–146 (2006).
36. Jawien, J., Gajda, M., Olszanecki, R. & Korbut, R. BAY x 1005 attenuates atherosclerosis in apoE/LDLR—Double knockout mice. *J. Physiol. Pharmacol.* **58**, 583–588 (2007).
37. Poeckel, D., Berry, K. A. Z., Murphy, R. C. & Funk, C. D. Dual 12/15- and 5-lipoxygenase deficiency in macrophages alters arachidonic acid metabolism and attenuates peritonitis and atherosclerosis in ApoE knock-out mice. *J. Biol. Chem.* **284**, 21077–21089 (2009).
38. Gaztanaga, J. *et al.* A phase 2 randomized, double-blind, placebo-controlled study of the effect of VIA-2291, a 5-lipoxygenase inhibitor, on vascular inflammation in patients after an acute coronary syndrome. *Atherosclerosis* **240**, 53–60 (2015).
39. Matsumoto, S. *et al.* Effect of treatment with 5-lipoxygenase inhibitor VIA-2291 (atreleuton) on coronary plaque progression: a serial CT angiography study. *Clin. Cardiol.* **40**, 210–215 (2017).
40. Matsukawa, A. *et al.* Endogenous monocyte chemoattractant protein-1 (MCP-1) protects mice in a model of acute septic peritonitis: cross-talk between MCP-1 and leukotriene B4. *J. Immunol.* **163**, 6148–6154 (1999).
41. Huang, L. *et al.* Leukotriene B4 strongly increases monocyte chemoattractant protein-1 in human monocytes. *Arterioscler. Thromb. Vasc. Biol.* **24**, 1783–1788 (2004).
42. Friedrich, E. B. *et al.* Mechanisms of leukotriene B4–triggered monocyte adhesion. *Arterioscler. Thromb. Vasc. Biol.* **23**, 1761–1767 (2003).
43. Xu, L. L., Warren, M. K., Rose, W. L., Gong, W. & Wang, J. M. Human recombinant monocyte chemotactic protein and other C-C chemokines bind and induce directional migration of dendritic cells in vitro. *J. Leukoc. Biol.* **60**, 365–371 (1996).
44. Gschwandtner, M., Derler, R. & Midwood, K. S. More than just attractive: how CCL2 influences myeloid cell behavior beyond chemotaxis. *Front. Immunol.* **10**, (2019).
45. Gerrity, R. G. & Naito, H. K. Lipid clearance from fatty streak lesions by foam cell migration. *Artery* **8**, 215–219 (1980).
46. Moore, K., Sheedy, F. & Fisher, E. Macrophages in atherosclerosis: A dynamic balance. *Nat. Rev. Immunol.* **13**, 709–721 (2013).
47. Spanbroek, R. *et al.* Expanding expression of the 5-lipoxygenase pathway within the arterial wall during human atherogenesis. *Proc. Natl. Acad. Sci. USA* **100**, 1238–1243 (2003).
48. Sánchez-Galán, E. *et al.* Leukotriene B4 enhances the activity of nuclear factor-kappaB pathway through BLT1 and BLT2 receptors in atherosclerosis. *Cardiovasc. Res.* **81**, 216–225 (2009).
49. Kaartinen, M., Penttilä, A. & Kovanen, P. T. Accumulation of activated mast cells in the shoulder region of human coronary atheroma, the predilection site of atheromatous rupture. *Circulation* **90**, 1669–1678 (1994).
50. Hellings, W. E. *et al.* Histological characterization of restenotic carotid plaques in relation to recurrence interval and clinical presentation: a cohort study. *Stroke* **39**, 1029–1032 (2008).
51. Butler, A., Hoffman, P., Smibert, P., Papalexi, E. & Satija, R. Integrating single-cell transcriptomic data across different conditions, technologies, and species. *Nat. Biotechnol.* **36**, 411–420 (2018).

52. Stuart, T. *et al.* Comprehensive integration of single-cell data. *Cell* **177**, 1888-1902.e21 (2019).
53. Hafemeister, C. & Satija, R. Normalization and variance stabilization of single-cell RNA-seq data using regularized negative binomial regression. *Genome Biol.* **20**, 1–15 (2019).
54. Stuart, T., Hoffman, P. & Satija, R. Seurat Signac Package. (2020).
55. Bot, I. *et al.* Mast cell chymase inhibition reduces atherosclerotic plaque progression and improves plaque stability in ApoE$^{-/-}$ mice. *Cardiovasc. Res.* **89**, 244–252 (2011).
56. Chomczynski, P. & Sacchi, N. Single-step method of RNA isolation by acid guanidinium thiocyanate-phenol-chloroform extraction. *Anal. Biochem.* **162**, 156–159 (1987).

Acknowledgements

The authors would like to thank Robin A.F. Verwilligen and Virginia Smit for technical assistance.

Author contributions

Conceptualization, M.A.C.D. and I.B.; data acquisition, M.A.C.D., F.D.V., E.H., L.D., M.N.A.B., P.S., A.C.F. and I.B.; data analysis and interpretation, M.A.C.D., F.D.V. and I.B.; writing—original draft preparation, M.A.C.D., F.D.V. and I.B.; writing—review and editing, all authors; funding acquisition, A.C.F., J.K. and I.B. All authors have read and agreed to the published version of the manuscript.

Funding

This research was funded by The Dutch Heart Foundation, grant number CVON2017-20: Generating the best evidence-based pharmaceutical targets and drugs for atherosclerosis (GENIUS II). M.A.C.D., I.B., J.K. are supported by the NWO-ZonMW (PTO program grant number 95105013). A.C.F. is supported by the Dutch Heart Foundation (2018T051). I.B. is an Established Investigator of the Dutch Heart Foundation (2019T067).

Competing interests

The authors declare no competing interests.

Additional information

Supplementary Information The online version contains supplementary material available at https://doi.org/10.1038/s41598-022-23162-4.

Correspondence and requests for materials should be addressed to I.B.

Reprints and permissions information is available at www.nature.com/reprints.

Publisher's note Springer Nature remains neutral with regard to jurisdictional claims in published maps and institutional affiliations.